Anomalous dispersion in a solid, silica-based fiber

S. Ramachandran, S. Ghalmi, J. W. Nicholson, M. F. Yan, P. Wisk, E. Monberg, and F. V. Dimarcello

OFS Laboratories, 19 Schoolhouse Road, Somerset, New Jersey 08873

Received March 22, 2006; revised May 15, 2006; accepted May 31, 2006;
posted June 19, 2006 (Doc. ID 69250); published August 9, 2006

We demonstrate an all-solid (nonholey), silica-based fiber with anomalous dispersion at wavelengths where silica material dispersion is negative. This is achieved by exploiting the enhanced dispersion engineering capabilities of higher-order modes in a fiber, yielding +60 ps/nm km dispersion at 1080 nm. By coupling to the desired higher-order mode with low-loss in-fiber gratings, we realize a 5 m long fiber module with a 300 fs/nm dispersion that yields a 1 dB bandwidth of 51 nm with an insertion loss of ~0.1 dB at the center wavelength of 1080 nm. We demonstrate its functionality as a critical enabler for an all-fiber, Yb-based, mode-locked femtosecond ring laser.

OCIS codes: 060.2280, 060.5530.

Generation of visible supercontinua, and several other fiber-based devices or applications such as soliton propagation, pulse compression, and building fiber laser cavities require fibers with anomalous dispersion ($D>0$ or $\beta_2<0$). In the entire wavelength range below 1300 nm, where silica material dispersion is negative, this has remained an unfulfilled aim of conventional silica-based fibers. Small-core microstructured optical fibers (MOF) have generated much interest due to their ability to achieve positive dispersion in this wavelength range.[1] However, aside from being technologically more complex than solid fibers, their design space is fundamentally limited by a trade-off between (positive) dispersion and A_{eff}. For instance, designs yielding dispersion $>+50$ ps/nm km at $\lambda\sim1060$ nm have[2] A_{eff} of $2-5$ μm^2. This would be advantageous for supercontinuum generation but may limit its utility in many applications as linear dispersive elements. Bandgap fibers are a promising alternative, but the bandgaps as well as loss are sensitive functions of the magnitude and geometry of their high-index regions.[3] It is conceivable that this technology will improve with time, but it is expected that the fabrication complexity and sensitivity of bandgap-guided fibers will always be higher than that of index guided fibers (such as standard fibers and MOFs).

In this Letter, we demonstrate what we believe to be the first all-solid, silica-based, index-guided fiber that can achieve anomalous dispersion at a variety of wavelengths below 1300 nm where silica material dispersion is negative. The key to the design is the ability to achieve strong positive waveguide dispersion for the LP_{02} mode of a specially designed higher-order-mode (HOM) fiber. This concept is unique to HOMs, and the conventional fundamental (LP_{01}) mode in single-mode fibers (SMFs) cannot access this design space because its waveguide dispersion is typically negative. We demonstrate a fiber that has +60 ps/nm km dispersion for the LP_{02} mode in the 1060 nm wavelength range. Low-loss long-period fiber gratings (LPG) enable coupling to the LP_{02} mode with >90% efficiency over a 51 nm bandwidth, with peak coupling efficiencies as high as 99.8%. Using a pair of such LPGs, we demonstrate a module with 5 m of HOM fiber that has conventional LP_{01} inputs and outputs, thus enabling integration with other fiber-based devices or systems. The total module loss, including splices, gratings, and propagation loss in the fiber, is only ~0.1 dB at the peak transmission wavelength of 1080 nm. We demonstrate the functionality of this fiber with a Yb-fiber-based mode-locked femtosecond ring laser.

The dispersion of a mode is roughly the sum of waveguide and material contributions. To achieve positive dispersion for $\lambda<1300$ nm where the material dispersion (D_m) of silica is negative, waveguide dispersion (D_w) needs to be strongly positive. Figure 1 provides the intuitive picture for the dispersive behavior of guided modes. Figure 1 is a schematic and simulated representation of modal behavior for the conventional LP_{01} (top), and the LP_{02} (bottom) modes in a fiber. Figure 1(a) shows the evolution of these mode profiles as a function of wavelength. The LP_{01} mode monotonically transitions from the high-index central core to the surrounding lower-index regions. Thus the fraction of power traveling in lower-index regions increases with wavelength. Since the velocity of light increases as the index of the medium drops,

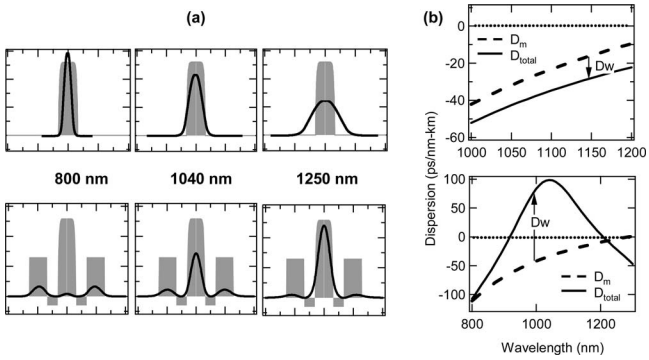

Fig. 1. Comparison of modal behavior between conventional LP_{01} (top, schematic) and LP_{02} (bottom, simulated) modes. (a) Mode profile versus λ, conventional mode transitions from high to low index; designed HOM shows opposite evolution. Gray background denotes index profile of the fiber; (b) Resultant total dispersion (solid). Also shown are silica material dispersion (D_m, dashed) and zero-dispersion line (dotted). Arrows show the contribution of waveguide dispersion (D_w) to total dispersion.

0146-9592/06/172532-3/$15.00

the LP_{01} mode experiences smaller group delays as wavelength increases. Waveguide dispersion (D_w), which is the derivative of group delay with respect to wavelength, is thus negative for the LP_{01} mode. In wavelength ranges in which D_m is itself negative, the conventional LP_{01} mode can achieve only negative dispersion values. This is illustrated in Fig. 1(b) (top), which plots material as well as total dispersion of the LP_{01} mode in the 1060 nm wavelength range. Note that this discussion is for the conventional LP_{01} mode in low-index-contrast waveguides that can be realized by conventional fiber fabrication techniques. The LP_{01} mode can, in fact, be designed to have large positive waveguide dispersion when the waveguide is tightly confining, such as in MOFs, where the air–silica boundary defines the confinement layer. For such waveguides, modal expansion with wavelength as depicted in Fig. 1(a) is negligible, and the waveguide dispersion is akin to that of microwave waveguides with perfectly reflecting waveguide walls. Hence large positive waveguide dispersion may be realized by tightly confined LP_{01} modes in MOFs, but the associated trade-off is with A_{eff}, and designs that yield dispersion $>+50$ ps/nm km in the wavelength ranges of 800 or 1060 nm typically have A_{eff} of $2-5\ \mu m^2$.

In contrast, the LP_{02} mode may be designed to have the mode evolution shown in Fig. 1(a) (bottom). As the wavelength of operation increases, the mode evolves in the opposite direction, in that the mode transitions from the lower-index regions to the higher-index core. By the intuition described in the previous paragraph, we infer that this mode will have $D_w > 0$. This is illustrated in Fig. 1(b) (bottom), which shows that in the wavelength range where this transition occurs, very large, positive values of D_w vastly exceeding the magnitude of (negative) D_m are obtained. This yields a mode with positive dispersion. Note that this evolution is governed by the "attractive" potential of various high-index regions of the waveguide and can thus be modified to achieve a variety of dispersion magnitudes, slopes, and bandwidths, much as DCFs can be designed to achieve a variety of negative dispersion values.[4,5]

Figure 2(a) shows the index profile of the fiber in this report—the broad, low-index ring serves to substantially guide the LP_{02} mode at shorter wavelengths, and the mode transitions to the small, high-index core as wavelength increases [see Fig. 1(a) for an example of this mode evolution]. The experimentally recorded near-field image of this mode [Fig. 2(b)] reveals that it has $A_{\text{eff}} \sim 44\ \mu m^2$ at 1080 nm. Figure 2(c) shows the schematic of the module, depicting LPGs at the input and output of the fiber, respectively. The LPGs are induced in the fiber by exposing the deuterium-loaded fiber to 248 nm UV light through an amplitude mask of a 225 μm grating period and a 2.5 cm length. They offer >90% conversion over a 51 nm bandwidth because, with peak coupling efficiencies of 99.8%, LPGs are typically very efficient mode converters but with bandwidths of only a few nm. We achieve the broad bandwidth by designing

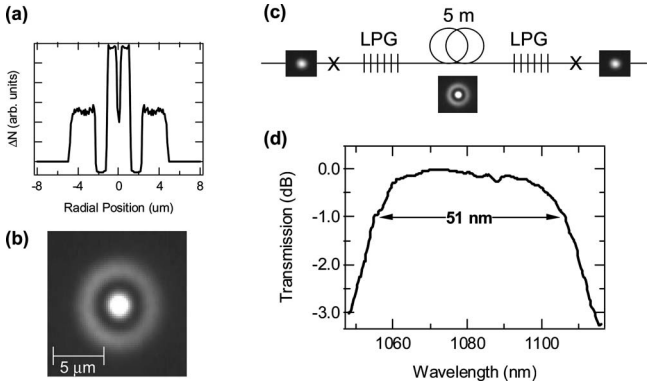

Fig. 2. (a) Index profile of HOM fiber and (b) experimentally imaged near-field image of LP_{02} mode with A_{eff} $44\ \mu m^2$. (c) Schematic of HOM dispersive module—input-output LPGs ensure device is compatible with conventional fibers. (d) Device transmission, 51 nm bandwidth and 0.1 dB total insertion loss at 1080 nm.

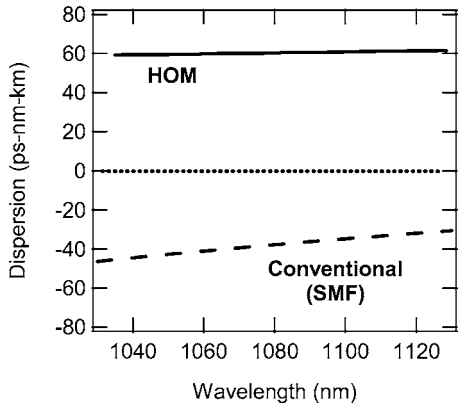

Fig. 3. Dispersion of HOM (solid line), compared with dispersion of conventional SMF (dashed line), measured by spectral interferometry. Also shown is the zero-dispersion line (dotted line).

the fiber to yield identical group velocities for the two coupled modes (the incoming LP_{01} and the converted LP_{02} mode) at the resonant wavelength of interest—this yields very broad bandwidths without the need for chirping or otherwise altering the profile of the grating.[4,6] This yields a 5 m HOM fiber module that has a 1 dB bandwidth of 51 nm [Fig. 2(d)]. The transmission plot includes all the loss contributions—splices to SMF pigtails, LPGs, and 5 m of HOM fiber—and illustrates a device loss of only 0.1 dB at the center wavelength of 1080 nm. This indicates that the device losses are governed primarily by the losses from conventional splices, and hence devices with losses <0.5 dB should be achievable in a repeatable fashion. No change in the transmission characteristics are observed when the HOM fiber is bent down to radii of 1 cm, indicating robust, mode-coupling-free light propagation in these fibers.

Figure 3 shows the central parameter of interest—the dispersion of the LP_{02} mode, as measured by spectral interferometry.[7] The dispersion, calculated from a first-order (linear) fit to the relative group delays, is +60 ps/nm km at 1080 nm. Also illustrated is the dispersion of a conventional SMF, which is nega-

tive in this wavelength range. This illustrates what we believe to be the first silica-based, index-guided solid fiber that yields anomalous dispersion in the 1060 nm wavelength range. The A_{eff} of this fiber (44 μm^2) is an order of magnitude larger than that of the MOFs with similar dispersion (MOF $A_{\text{eff}} \sim 4$ μm^2), and is, in fact, larger than that of commercial SMFs at these wavelengths (SMF $A_{\text{eff}} \sim 32$ μm^2).

Fiber lasers in the 1060 nm wavelength range require a positive dispersion element to obtain a cavity with net dispersion nominally equal to zero. This is because the cavity primarily comprises conventional fibers with negative dispersion. This is normally achieved by using highly lossy bulk-optic gratings or small A_{eff} MOFs. Here, we use the low-loss, large A_{eff} HOM fiber module of Fig. 2(c) as the positive dispersion element in a ring-fiber-laser cavity. The laser had a stretched-pulse ring configuration [Fig. 4(a)], with mode locking based on nonlinear polarization evolution.[8] A single-mode, 975 nm pump diode with up to 300 mW output power was coupled into a 1 m length of Yb-doped SMF. An isolator ensured unidirectional operation and a polarizer provided polarization-dependent loss. Mode locking was initiated by adjusting the polarization state of the cavity. Without the HOM fiber in the cavity, we were unable to initiate mode locking. With the HOM fiber in the cavity, we observed a stable pulse train [Fig. 4(b)], with an average output power of approximately 1 mW. The operating bandwidth of the laser was adjusted by trimming the length of SMF in the cavity, and consequently tuning the overall cavity dispersion. At a pulse repetition frequency of 18.5 MHz, the maximum observed spectral width was 28 nm [Fig. 4(c)], corresponding to a 61.7 fs bandwidth-limited Gaussian pulse. At the time of writing, an autocorrelator operating at 1 μm was unavailable.

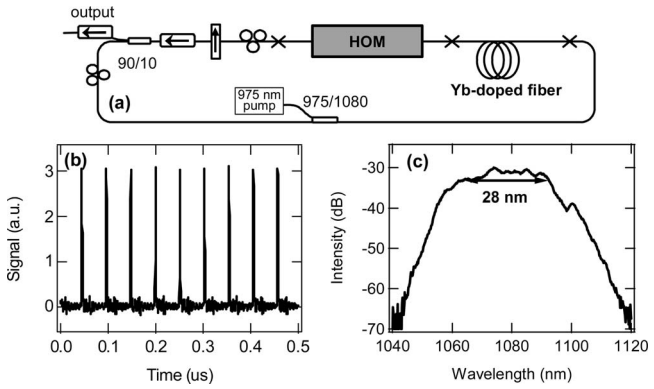

Fig. 4. (a) Schematic of stretched-pulse ring laser in which the HOM module is used as the positive dispersion element, (b) typical mode-locked pulse train, (c) spectrum of output pulse: 3 dB width ~28 nm.

In summary, we demonstrate a silica-based, solid (nonholey) fiber that yields strong positive waveguide dispersion, which leads to what we believe to be the first demonstration of anomalous dispersion for $\lambda < 1300$ nm from an index-guided, all-solid, silica-based fiber. In this wavelength range, the material dispersion of silica forces conventional fibers to have negative dispersion. The key enabler is the unique design flexibility of higher-order modes in a fiber. Combined with in-fiber gratings, this enables construction of positive dispersion elements with a bandwidth of 51 nm, low loss (~0.1 dB), and A_{eff} (44 μm^2) that is an order of magnitude larger than the alternative (MOF). We demonstrate its functionality by using it as a positive dispersion element to achieve mode locking in a stretched-pulse ring laser that yielded femtosecond pulses with a 28 nm bandwidth.

We expect that this demonstration will have far reaching implications for the design of fiber-based short-pulse devices in the visible and near-IR wavelength ranges, because this fiber provides the low-loss, bend- and nonlinearity-resistant operation of conventional fibers in a wavelength range where conventional fibers cannot achieve anomalous dispersion.

The authors thank J. Fini for help with calculating the dispersion in MOFs. This work was performed with the support of the U.S. Department of Commerce, National Institute of Standards and Technology, Advanced Technology Program, Cooperative Agreement 70NANB4H3035. S. Ramachandran's e-mail address is sidr@ieee.org.

References

1. J. C. Knight, J. Arriaga, T. A. Birks, A. Ortigosa-Blanch, W. J. Wadsworth, and P. St. J. Russell, IEEE Photon. Technol. Lett. **12**, 807 (2000).
2. The MOF dispersion was approximated by calculations of dispersion in thin silica rods.
3. J. Riishede, J. Lægsgaard, J. Broeng, and A. Bjarklev, J. Opt. A, Pure Appl. Opt. **6**, 667 (2004).
4. S. Ramachandran, J. Lightwave Technol. **23**, 3426 (2005).
5. L. Gruner-Nielsen, M. Wandel, P. Kristensen, C. Jørgensen, L. V. Jørgensen, B. Edvold, B. Pálsdóttir, and D. Jakobsen, J. Lightwave Technol. **23**, 3566 (2005).
6. S. Ramachandran, Z. Wang, and M. F. Yan, Opt. Lett. **27**, 698 (2002).
7. D. Menashe, M. Tur, and Y. Danziger, Electron. Lett. **37**, 1439 (2001).
8. K. Tamura, E. Ippen, H. Haus, and L. Nelson, Opt. Lett. **18**, 1080 (1993).